Adsorption and coadsorption of single and multiple natural organic matter on Ag (111) surface: A DFT-D study

Nangamso Nathaniel Nyangiwe[1,2*], Cecil Naphtaly Moro Ouma[1,3]

[1]Natural Resources and the Environment, Council for Scientific and Industrial Research (CSIR), P O BOX 395, Pretoria, 0001, South Africa.
[2]University of Pretoria, Department of Chemical Engineering, Private Bag X 20, Hatfield, 0028, South Africa.
[3]HySA-Infrastructure, North-West University, Faculty of Engineering, Private Bag X6001, Potchefstroom, 2520, South Africa

Highlights

- The competitive adsorption between different NOM's on Ag (1 1 1) surface was investigated.
- The adsorption energy results suggest that the more the NOM's on Ag (1 1 1) surface, the higher the adsorption.
- The global reactivity descriptors in the gas phase and water as a solvent were calculated.

Abstract

The nature of the interaction of low molecular weight natural organic matter (NOM) with the Ag (111) surface is of crucial importance in the environment. The low molecular weight organics used in this study are formic acid (FA), acetic acid (AA1) and ascorbic acid (AA2). In this study, we think of a realistic environment where single, multiple or even a mixture of NOM's can attach on one Ag (111) surface. Such critical information is relevant in order to understand the behaviour of engineered nanoparticles (ENPs) when they get into the environment. To bridge this gap, we investigate the adsorption and co-adsorption properties of NOM's on Ag (111) surface using dispersion-corrected density functional theory (DFT-D) in the gas phase and water as a solvent. Throughout this paper, the number behind the letter represents the number of molecules i.e nFA, nAA1, nAA2 (n=1,2,3,4).The results of the calculated adsorption energy suggest that the interaction of 4FA, 2AA1 and 2AA2 molecules with Ag (111) surface is the strongest with the most negative values (-6.54 and -3.84 eV) in both gas phase and COSMO respectively which reveals that is the most stable system.The global reactivity descriptors in the gas phase and water as a solvent were calculated.

Graphical abstract

Side and top view snapshot of Ag (1 1 1)-1AA2, Ag (1 1 1)-2AA2 and Ag (1 1 1)-3AA2.

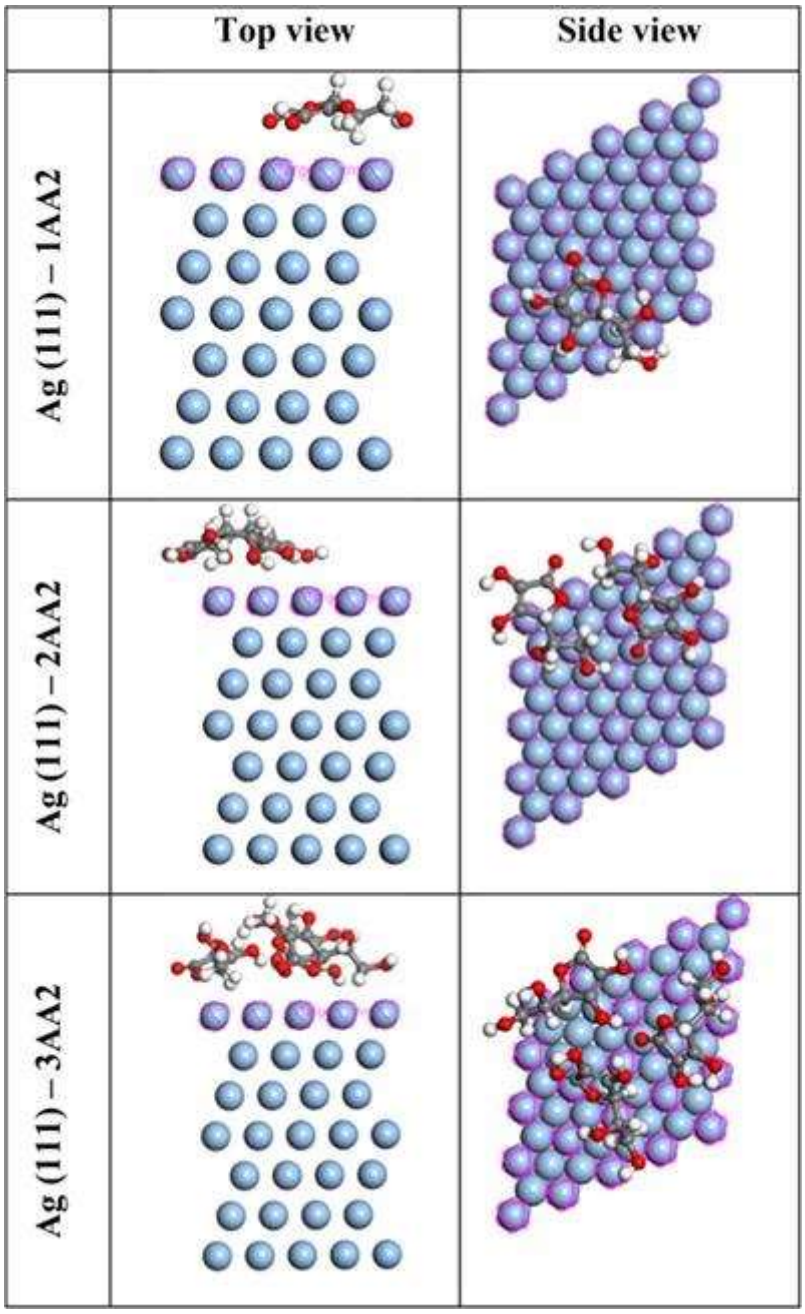

Keywords: DFT-D, Ag (111) surface, interaction, adsorption, coadsorption, natural organic matter

1. Introduction

The nanotechnology field continues to grow rapidly and the increasing use of engineered nanoparticles (ENPs) in commercial products translates into an increasing presence in the biosphere. Engineered NMs are manufactured materials having at least one dimension in the nanoscale (1−100 nm) dimension [1]. Once released into the environment, silver engineered nanoparticles (Ag ENPs)

undergo different pathways during transportation. They may remain as individual particles in suspension and be delivered long distances, or tend to aggregate at high ionic strength [2,3]. After contact with oxygen and other oxidants, partial oxidation and Ag+ dissolution is also expected. Most probably, Ag ENPs would react with sulfides, chlorides or other natural substances, altering the original properties of the nanoparticles [4,5]. The behaviours of the Ag ENPs largely depends on the surface properties of the nanoparticles themselves and the surrounding environment, involving capping agents, electrolyte composition, solution ionic strength, pH and NOM [6-8]. NOM is expected to attach to the surface of ENPs, changing the physiochemical properties of ENPs and the interfacial forces or energies between interacting ENPs, thereby altering the aggregation behaviour [9,10]. Various experimental studies have shown that the pH, ionic strength, electrolyte valence, and NOM content of an aquatic system control the surface charge and aggregation state of ENPs [11-13]. In these studies, NOM has been found to influence ENPs stability and surface chemistry for carbon-based nanomaterials and metals. However, increased production levels inevitably lead to increasing incidence of the materials in the environment. Until a few years ago, little was known about the fate of nanomaterials in the environment. Recent studies suggest important emerging patterns [14-16]. There are still major knowledge gaps for even the most widely used ENPs involving their postproduction life cycles. This includes entry into the environment, environmental pathways, eventual environmental fate, and potential ecotoxicological effects. The adsorption of NOM to the surfaces of natural colloids and engineered nanoparticles is known to strongly influence, and in some cases control their surface properties and aggregation behaviour. The adsorption process of molecules at the surface can be computed by ab initio calculations, which have been proven to be a useful tool to understand the gas-sensing mechanism at atomic level [17]. As a result, the understanding of nanoparticle fate, transport and toxicity in natural systems must include a fundamental framework for predicting such behaviour.

ENPs may enter the environment intentionally (e.g., use of zero valent iron NPs for remediation) or by accidental release (e.g., release of silver ions after washing socks embedded with Ag ENPs [18-19]. Toxicologists have demonstrated the uptake, accumulation, and toxicity of nanomaterials in organisms exposed to ENPs [20]. Moreover, effects on organisms are dependent on nanomaterial physicochemical properties [20]. The ENPs physicochemical properties will be influenced by environmental conditions and it is critical to assess environmental behaviour of these materials to gain an understanding of the possible implications. These properties will also influence their environmental behaviour, hence there is an urgent need to determine the effects of ENPs surface functionality on their behaviour in aquatic systems, including interactions with NOM's.

According to literature, the physicochemical properties of ENPs and the characteristics of NOM's will determine the extent of adsorption and the influence on stability [21,22]. There is a need to correlate environmental behaviour with specific properties of ENPs and aquatic chemical composition (including NOM) for development of predictive models to assess the environmental impacts of ENPs. A library of well-defined ENPs with varying surface chemistry is essential to gain an understanding of the relationship between ENP physicochemical characteristics and their behaviour in environmental

systems [8,23,24]. As engineers and scientists build models to predict the fate and transport of engineered ENPs in the environment, there is a need to relate properties of the ENPs with specific environmental behaviour. Building from our previous work [25],[26], the purpose of the paper is to gain insight on the adsorption and coadsorption of natural organic matter on Ag (111) surface. Thus the paper aimed at answering the following questions, can we adsorb more than one NOM on the Ag (111) surface? It is possible to coadsorb a mixture of NOM's on Ag (111) surface? The goal of this study is to further understand the Ag (111) surface adsorption and co-adsorption with low molecular weight (LWM).The investigations in this paper go beyond those in the current literature considering the implications of adsorption and co-adsorption of LMW NOMs mixtures on the surfaces of nAg (111) to establish the likely implications of a mixture of NOM's on the adsorption. Overall, this theoretical based-study attempts to offer better insights on how NOMs MW singularly and mixtures of NOMs co-existing in the aquatic system may influence the fate of ENPs. To the best of our knowledge, this is one of the few studies to provide insight to elucidate how a mixture of NOMs may have diverse set of implications on the fate of ENPs in aquatic systems using first-principles calculations; and may be a useful reference in designing experiments on the influence of different NOMs on the ENMs fate in aquatic systems. The use of density functional theory technique based on its strengths like non-intrusive, lesser laborious and not costly compared to experimental studies can be valuable tool to screen potential descriptors for ENPs interactions with NOM during the adsorption process. In this context, the results have potential significance in advancing the field of risk assessment of ENPs in the aquatic systems, and enhancing the application of DFT in other fields of science.

2. Computational details

All of the spin-polarized calculations were performed within density functional theory dispersion-corrected (DFT-D) computations as implemented in DMol3 code embedded in Materials Studio (Accelrys, San Diego, CA) [27]. The generalized gradient approximation (GGA) with Perdew–Burke–Ernzerhof (PBE) functional was employed using the DFT semi-core pseudopotential [28] to describe exchange and correlation effects and the polarization p-function (DNP) as the basis set for the double numerical atomic orbital augmented was chosen. The convergence tolerances of the geometry optimization are set to 10^{-5} Ha (1 Ha = 27.21 eV) for the energy, 0.002 Ha for the maximum force, and 0.005 Å for the maximum displacement. The electronic SCF tolerance is set to 10^{-6} Ha. In order to achieve accurate electronic convergence, we apply a smearing of 0.005 Ha to the orbital occupation. Convergence accuracy of charge density of self-consistent field was 1.0^{-6} Ha and Brillouin k point was 1×1×1. In addition, direct inversion of iterative subspace (DIIS) was chosen to accelerate convergence speed of charge density of self-consistent field to reduce calculation time and enhance efficiency. A Fermi smearing of 0.005 hartree and a real-space cutoff of 4.4 Å were employed to improve the computational performance. The Ag (111) surface was modelled using a seven-layer slab with a (4×4) unit cell and only the top three layers were allowed to relax while the four bottom layers were fixed in the optimized bulk position. A 20 Å vacuum space between the periodic slabs was utilized to eliminate spurious interactions. The effect of solvent was modelled by COSMO [29], where water has been used as a solvent. COSMO is a considerable simplification of the continuum solvation

model without significant loss of accuracy [30]. For solvation studies, water which has the highest dielectric constant (78.4), is taken as solvating medium as it mimics the human biological system in recognizing the behaviour of NOM's on Ag (111) surface in aquatic systems in the environment

Ag ENPs exhibits different shapes such as cubooctahedral, multiple-twinned decahedral, quasispherical shape with pre-dominant (100) facets along a small percentage of (111) facets and rod-like shapes e.g., pentagonal rods which have side surfaces and ends, respectively, bounded by (100) facets and (111) facets [31]. Previously Pal et al [32], and colleagues investigated the effects of Ag ENPs and showed shape-dependent interactions with Escherichia coli primarily due to marked differences in reactivity of different crystal facets. In particular, the (111) facet was found to have induced the most significant antibacterial activity linked to high atoms density [32]. Similarly, Morones et al [33] demonstrated increased Ag ENPs toxicity to several bacterial strains linked to higher reactivity presented by the (111) facets. In addition, the adsorption of NOM's onto different surfaces and different shapes of NPs is likely to play a significant role in elucidating the NPs' transport and fate in the environment [34].

Figures 1-5 show the optimized structures of side and top view snapshot. Throughout this section, the number behind the letter represent the number of molecules i.e. nFA, nAA1, nAA2.

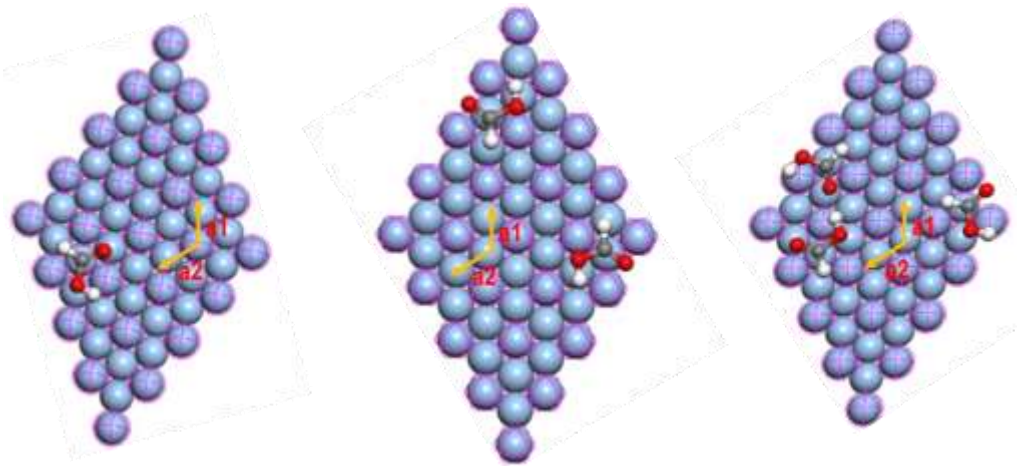

Figure 1: Side view crystallographic axes snapshot of Ag (111)-1FA, Ag (111)-2FA and Ag (111)-3FA

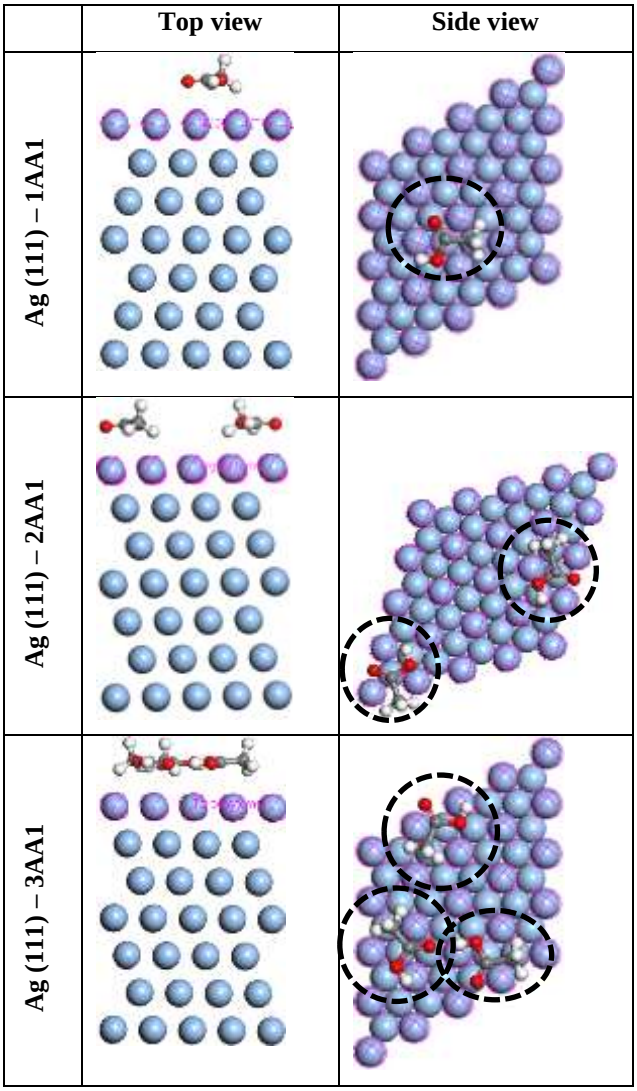

Figure 2: Side and top view snapshot of Ag (111)-1AA1, Ag (111)-2AA1 and Ag (111)-3AA1

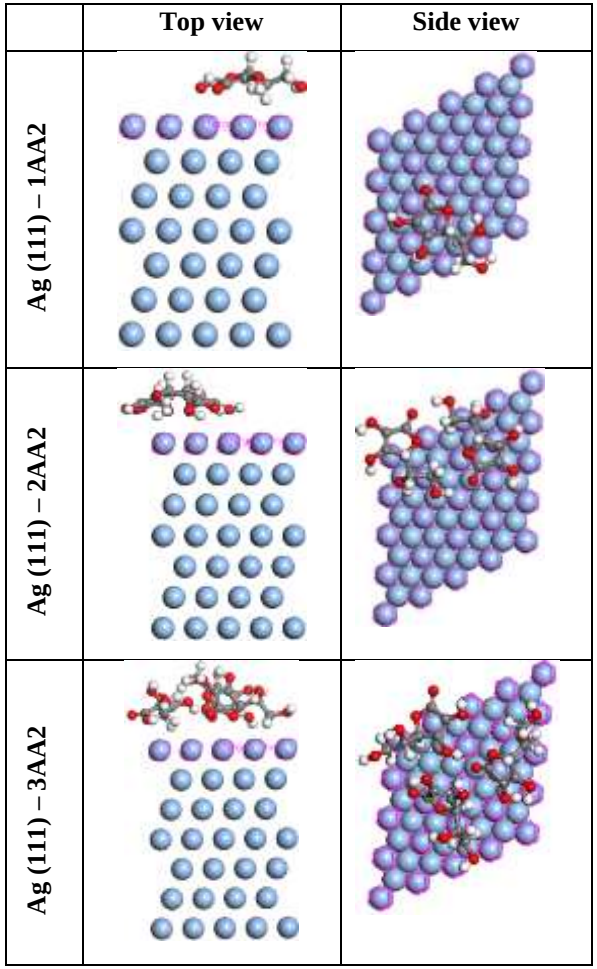

Figure 3: Side and top view snapshot of Ag (111)-1AA2, Ag (111)-2AA2 and Ag (111)-3AA2.

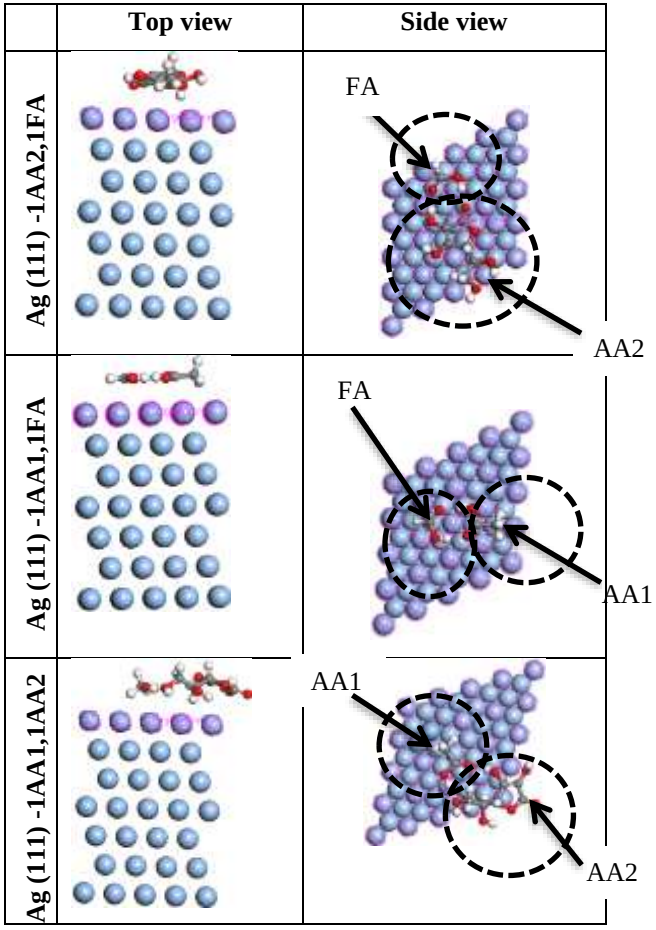

Figure 4: Side and top view snapshot of Ag (111)-1AA2, Ag (111)-2AA2 and Ag (111)-3AA2.

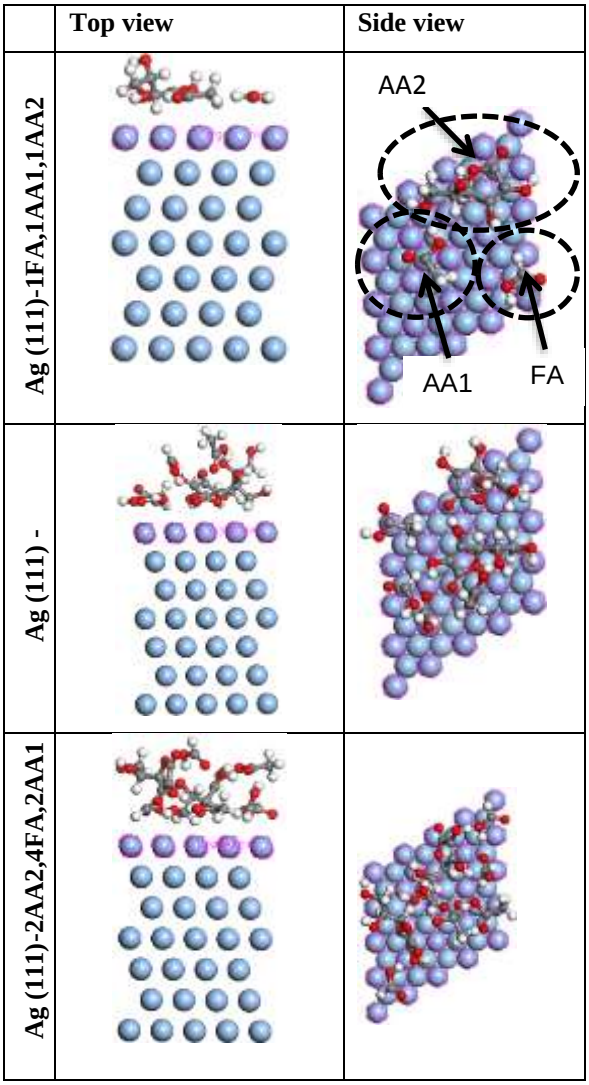

Figure 5: Side and top view snapshot of Ag (111)-1AA2, 1FA, Ag (111)-1AA1,1FA and Ag (111)-2AA2,4FA,2AA1.

3. Results and discussion

3.1 Adsorption and co-adsorption of one, two, three and a mixture of different NOM's on Ag (111) surface

This adsorption and co-adsorption study was motivated by the fact that in a real environment, it is highly possible for single, multiple or even a mixture of different NOM to attach on one Ag (111) surface at the same time, thus a realistic environmental scenario has been mimicked. This study has suggested that it is possible to adsorb more than one NOM on the Ag (111) surface using computational modelling. After optimization, the adsorption and co-adsorption configurations of 1AA1, 2AA1 and 3AA2 on Ag (111) surface were obtained, as presented in Figures 1-5. The adsorption and co-adsorption energies are shown in Table 1 were obtained from the expression.

$$E_{ads} = E_{NOM/surface} - nE_{NOM} - E_{surface} \quad (1)$$

$E_{NOM/surface}$ is the total energy of the surface and the NOM, where E_{NOM} is the energy of the NOM without the surfaceand $E_{surface}$ is the energy of the surface without the adsorbate. In the expression above, *n* is the number of adsorbates on the Ag (111) surface.

Table 1: Adsorption and coadsorption of NOM's on Ag (111) surface and equilibrium distance in gas phase and in water as a solvent as well as molecular weights.

System	MW g/mol	Eads (eV) gas phase	dH-Ag (Å) gas phase	dO-Ag (Å) solvent	Eads (eV) solvent	dH-Ag (Å) solvent	dO-Ag (Å) solvent
Ag (111)-1FA	46.02	-0.19	5.16	-	-0.07	5.16	-
Ag (111)-2FA	92.02	-1.38	5.23	-	-0.49	-	5.22
Ag (111)-3FA	138.06	-1.81	-	5.18	-0.65	5.18	5.18
Ag (111)-1AA1	60.05	-0.32	4.46	-	-0.17	4.46	-
Ag (111)-2AA1	120.1	-1.52	4.43	-	-0.61	4.43	-
Ag (111)-3AA1	180.15	-2.06	4.44	-	-0.90	4.44	-
Ag (111)-1AA2	176.12	-0.53	3.57	-	-0.32	4.30	-
Ag (111)-2AA2	352.24	-3.05	3.77	-	-1.63	3.77	-
Ag (111)-3AA2	528.36	-3.77	3.90	-	-1.72	3.59	-
Ag (111)-1AA1,IFA	106.07	-2.29	4.05	-	-1.32	3.86	-
Ag (111) -1AA2,1FA	222.14	-4.41	3.80	-	-2.49	3.91	-
Ag (111) -1AA1,1AA2	236.17	-2.06	3.63	-	-0.80	3.85	-
Ag (111)- 1FA,1AA1,1AA2	282.19	-1.92	3.61	-	-1.10	3.61	-
Ag (111) -2FA,2AA1,2AA2	564.38	-1.00	4.42	-	-0.55	4.42	-
Ag (111)-4FA,2AA1,2AA2	656.42	-6.54	3.36	-	-3.84	3.75	-

According to Table 1, our computations, both gas phase and COSMO results reveal that the adsorption and co-adsorption of NOM's on Ag (111) surface is favourable. As shown in Table 1, the adsorption and co-adsorption energy becomes stronger as the number of molecules increases on the Ag (111) surface. The adsorption energy of 3AA2 on Ag (111) surface is the most negative value -3.77 eV and -1.72 eV respectively in the gas (solvent) phase. From Table 1, an increase in equilibrium distances between the Ag (111) surface and NOM's as the adsorption energy increases 3.90 Å and 3.59 Å in gas and water phase has been observed. Another trend was observed for the co-adsorption with the exception of 1FA, 1AA1, 1AA2 on Ag (111) surface, the reason for these molecules to have less adsorption energy could be attributed to the fact that molecules with unique properties such as, molecular weight, electronegativity melting point etc. when put on one surface are likely to compete for the active adsorption sites.

When the system consists of adsorbates with different molecular properties, the difference in interaction energies will lead to enhancement of one adsorbate relative to the others. Previous study by Timón et. al [35] while working on structural single and multiple molecular adsorption of CO_2 and H_2O in zeolitic imidazolate framework crystals dealt with the issue of competition, even though some of the molecules in their study were not favourable unlike in this study where all the molecules are favourable. Another study that dealt with the issue of competition was conducted by Nalaparaju et.al.

[36] on molecular understanding for the adsorption of water and alcohols in hydrophilic and hydrophobic zeolitic metal−organic frameworks. This study found that the adsorption energy increases as the number of molecules is increasing. For the co-adsorption results we observed that a mixture of 2AA2, 4FA and 2AA1 on Ag (111) has the highest adsorption energy -6.54 eV (-3.84 eV) respectively in the gas (solvent) phase making it the most stable compared to other mixtures of different NOM's. The equilibrium distances between the Ag (111) surface and NOM's were 3.36 Å and 3.75 Å respectively in the gas (solvent) phase. It has been observed that from individual adsorption energies of FA, AA1 and AA2, the adsorbate with the highest adsorption energy will adsorb first on the Ag (111) surface. In our case, AA2 has the highest adsorption energies compared to FA and AA1.

3.2 Electronic structure

Figure 6 reveals the charge distribution, HOMO and LUMO of FA, AA1 and AA2 in COSMO. The charge distribution, HOMO and LUMO of FA, AA1 and AA2 in gas phase are shown in Figure S1 (Supporting document)

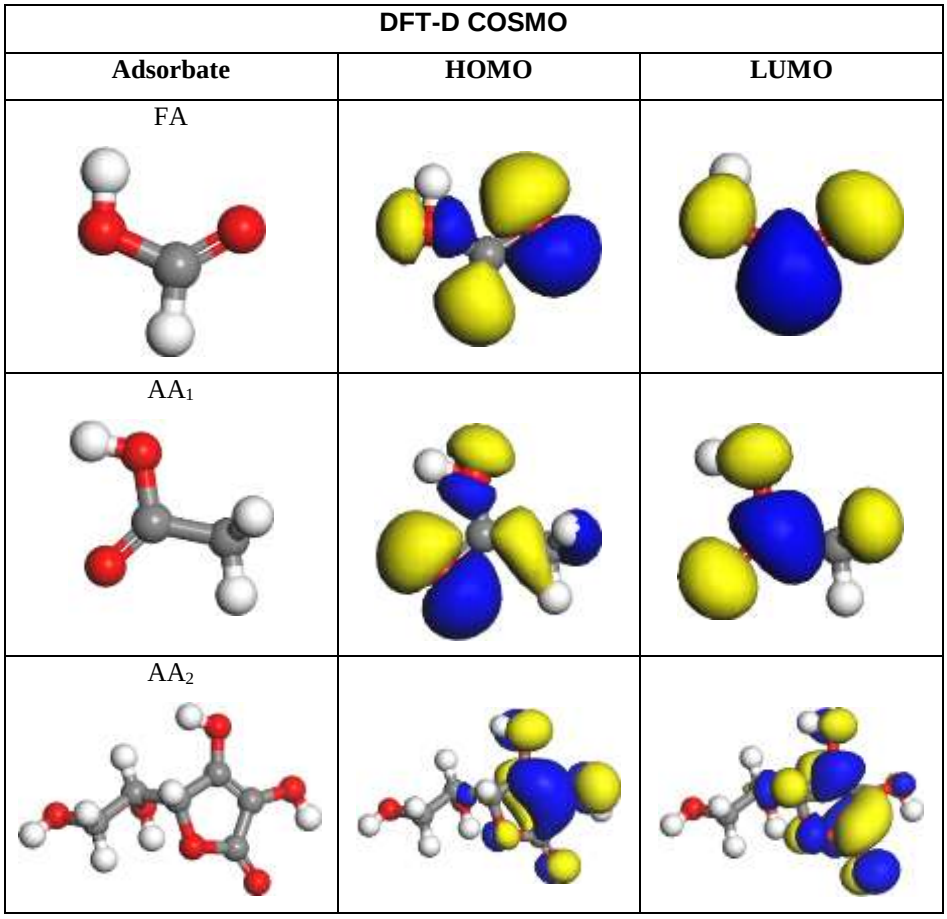

Figure 6: Optimized structures and the frontier molecular orbital density distributions (HOMO and LUMO) in COSMO.

To better understand the adsorption and co-adsorption process of NOM's on Ag (111) surface, frontier molecular orbitals (HOMO and LUMO) were analysed. The HOMO and LUMO for FA, AA1

and AA2 (Figure 6) show density uniformly distributed on all atoms. It is worth noting that going from gas phase to water as a solvent the HOMO and LUMO distribution slightly change as shown in Table 2 and 3. Tables 2-3 give the global reactivity descriptors calculated using equations in equation 2-5.

$$\chi = \frac{IP + EA}{2} \quad (2)$$

$$\eta = \frac{IP - EA}{2} \quad (3)$$

I and A are related in turn to E_{HOMO} and E_{LUMO} as $IP = -E_{HOMO}$, and $EA = -E_{LUMO}$

The chemical potential and electrophilicity index respectively are calculated as follows;

$$\mu = -\chi = (E_{HOMO} + E_{LUMO})/2 \quad (4)$$

$$\omega = \frac{\mu^2}{2\eta} \quad (5)$$

Based on Koopman's theorem [37], electronegativity (χ) and hardness (η) are related to electron affinity (EA) and ionization potential (IP)

Table 2: Calculated global reactivity descriptors (eV) in water as a solvent.

	DFT-D COSMO								
System	EHOMO	ELUMO	Eg	μ	IP	EA	χ	η	ω
FA	-6.89	-1.45	5.45	-4.17	6.89	1.45	4.17	2.72	3.19
AA1	-6.60	-1.14	5.46	-3.87	6.60	1.14	3.87	2.73	2.74
AA2	-5.64	-1.86	3.78	-3.75	5.64	1.86	3.75	1.89	3.72
Ag (111)	-4.50	-4.41	0.09	-4.46	4.50	4.41	4.46	0.04	228.15
Ag (111)-1FA	-4.75	-4.48	0.27	-4.62	4.75	4.48	4.62	0.13	79.20
Ag (111)-2FA	-4.74	-4.46	0.27	-4.60	4.74	4.46	4.60	0.14	76.99
Ag (111)-3FA	-4.71	-4.44	0.28	-4.57	4.71	4.44	4.57	0.14	75.39
Ag (111)-1AA1	-4.50	-4.42	0.08	-4.46	4.50	4.42	4.46	0.04	251.60
Ag (111)-2AA1	-4.46	-4.39	0.07	-4.43	4.46	4.39	4.43	0.04	277.05
Ag (111)-3AA1	-4.71	-4.43	0.28	-4.57	4.71	4.43	4.57	0.14	75.30
Ag (111)-1AA2	-4.44	-4.38	0.06	-4.41	4.44	4.38	4.41	0.03	311.07
Ag (111)-2AA2	-4.66	-4.37	0.29	-4.52	4.66	4.37	4.52	0.14	70.74
Ag (111)-3AA2	-4.69	-4.40	0.29	-4.54	4.69	4.40	4.54	0.14	72.23
Ag (111)-1AA1,1FA	-4.73	-4.46	0.27	-4.60	4.73	4.46	4.60	0.14	76.90
Ag (111)-1AA2,1FA	-4.70	-4.42	0.28	-4.56	4.70	4.42	4.56	0.14	74.25
Ag (111)-1AA1,1AA2	-4.70	-4.43	0.27	-4.56	4.70	4.43	4.56	0.14	76.53
Ag (111)-1FA,1AA1,1AA2	-4.67	-4.38	0.29	-4.52	4.67	4.38	4.52	0.14	71.63
Ag (111)-2FA,2AA1,2AA2	-4.71	-4.40	0.31	-4.55	4.71	4.40	4.55	0.16	66.81
Ag (111)-4FA,2AA1,2AA2	-4.80	-4.51	0.29	-4.65	4.80	4.51	4.65	0.14	75.82

Table 3: Calculated global reactivity descriptors (eV) in the gas phase.

	DFT-D Gas phase								
System	EHOMO	ELUMO	Eg	μ	IP	EA	χ	η	ω
FA	-6.74	-1.43	5.31	-4.08	6.74	1.43	4.08	2.65	3.14
AA1	-6.29	-1.00	5.29	-3.65	6.29	1.00	3.65	2.65	2.51
AA2	-5.57	-1.78	3.79	-3.68	5.57	1.78	3.68	1.90	3.56
Ag (111)	-4.50	-4.41	0.09	-4.45	4.5	4.41	4.45	0.04	227.88
Ag (111)-1FA	-4.74	-4.47	0.27	-4.61	4.74	4.47	4.61	0.13	78.83
Ag (111)-2FA	-4.71	-4.43	0.27	-4.57	4.71	4.43	4.57	0.14	76.00
Ag (111)-3FA	-4.67	-4.40	0.27	-4.53	4.67	4.40	4.53	0.14	74.82
Ag (111)-1AA1	-4.47	-4.39	0.08	-4.43	4.47	4.39	4.43	0.04	248.54
Ag (111)-2AA1	-4.40	-4.33	0.07	-4.37	4.4	4.33	4.37	0.04	269.60
Ag (111)-3AA1	-4.63	-4.36	0.28	-4.50	4.63	4.36	4.50	0.14	72.81
Ag (111)-1AA2	-4.41	-4.35	0.06	-4.38	4.41	4.35	4.38	0.03	306.10
Ag (111)-2AA2	-4.57	-4.28	0.29	-4.42	4.57	4.28	4.42	0.14	68.48
Ag (111)-3AA2	-4.63	-4.33	0.30	-4.48	4.63	4.33	4.48	0.15	67.60
Ag (111)-1AA1,1FA	-4.69	-4.41	0.28	-4.55	4.69	4.41	4.55	0.14	74.67
Ag (111)-1AA2,1FA	-4.63	-4.35	0.28	-4.49	4.63	4.35	4.49	0.14	71.97
Ag (111)-1AA1,1AA2	-4.62	-4.34	0.28	-4.48	4.62	4.34	4.48	0.14	72.37
Ag (111)-1FA,1AA1,1AA2	-4.55	-4.28	0.27	-4.41	4.55	4.28	4.41	0.14	71.59
Ag (111)-2FA,2AA1,2AA2	-4.52	-4.22	0.30	-4.37	4.52	4.22	4.37	0.15	63.19
Ag (111)-4FA,2AA1,2AA2	-4.53	-4.23	0.30	-4.38	4.53	4.23	4.38	0.15	64.67

Moreover, we observed that the energy gap (Eg) decreased after adsorption. Previous studies [38-39] showed that lower Eg means higher electrical conductivity and in contrast higher Eg corresponds to the lower electrical conductivity. Relatively small changes after adsorption and co-adsorption (Table 2-3) in both gas phase and COSMO, Eg again indicate limited perturbation(s) on Ag (111) surface.

The calculated μ values in Table 2 for the Ag (111) surface indicate that after adsorption and co-adsorption with 1FA, 2FA and 3FA, the chemical potential increased from -4.46 to -4.62, -4.60 and -4.57 eV, respectively. In contrast, a different observation was made for the Ag (111) surface with 1AA1, 2AA1 and 3AA1, after adsorption and co-adsorption. The μ values remained the same at -4.46 eV, decreased to -4.43 eV and increased to -4.57 eV. Similar observation were made for the Ag (111) surface with 1AA2, 2AA2 and 3AA2 After adsorption and co-adsorption the μ values decreased from -4.46 to -4.41 for the 1AA2 surface and then increase for the 2AA2 and 3AA2 to 4.52 and -4.54 eV respectively. The adsorption of different NOM's on Ag (111) surface showed an increase in the values of μ from -4.46 eV for a pristine Ag (111) surface to -4.60, -4.56, -4.56, -4.52, -4.55 and -4.65 eV on Ag (111)-1AA1,1FA, Ag (111)-1AA2,1FA, Ag (111)-1AA1,1AA2, Ag (111)-1FA,1AA1,1AA2, Ag(111)-2FA,2AA1,2AA2 and Ag 111)-4FA,2AA1,2AA2 respectively.

Moving from water to gas phase, it has been observed in Table 3 that a similar trend after adsorption and co-adsorption was observed. The μ values increased from -4.47 eV for the Ag (111) surface pristine to -4.61, -4.57 and -4.53 eV for 1FA, 2FA and 3FA respectively. In the case of Ag (111)

surface with 1AA1, 2AA1 and 3AA1, after adsorption and co-adsorption, the μ values decreased and increased from -4.47 to -4.43, -4.37 and 4.50 eV, respectively. For the Ag (111) surface with 1AA2, 2AA2, 3AA2 after adsorption and co-adsorption the μ values decreased and increased from -4.47 to -4.29, -4.31 and -4.51 respectively. Unlike in water as a solvent, in the gas phase as shown in Table 3, the co-adsorption of different NOM's on Ag (111) surface showed an increase, decrease and increase again in the values of μ from -4.47 eV for the Ag (111) surface for the pristine before co-adsorption to -4.41, -4.59, -4.48, -4.49, -4.55 and -4.39 eV for Ag (111)-1FA,1AA1,1AA2, Ag (111) -2FA,2AA1,2AA2, Ag (111)-1AA1,1AA2, Ag(111)-1AA2,1FA, Ag(111)-1AA1,1FA and Ag(111)-2AA2,4FA,2AA1 respectively.

A close look at Table 2 the values of μ are very similar. The difference is very small even though the COSMO values are a bit higher than the μ values in gas phase except in the case of Ag (111) -2FA, 2AA1, 2AA2 where a μ value of -4.55 and -4.59 eV in the water as a solvent and in the gas phase respectively were observed. Based on the μ values obtained in Table 2 and Table 3, it can be concluded that water as the solvent enhances the reactivity. Compared to μ values, ionization potential also followed the same trend before and after adsorption and co-adsorption, increased, decreased, increased and decreased. In the case of EA, different results were observed. The EA values increase from 4.43 eV for the Ag (111) surface pristine to 4.48 eV and 4.46 eV for 1FA and 2FA respectively while they remain unchanged for 3FA at 4.43 eV. For other adsorption and co-adsorption as shown in Table 3, IP decreased except for Ag (111) -1AA1, 1FA where we observed 4.45 eV, after co-adsorption.

Similar to μ values and values for electronegativity (χ) after adsorption and co-adsorption with 1FA, 2FA and 3FA, the chemical potential increased. Something dissimilar for the Ag (111) surface with 1AA1, 2AA1 and 3AA1, after adsorption and co-adsorption the chemical potential (μ) values decreased and increased respectively. Similar observation was made for the Ag (111) surface with 1AA2, 2AA2 and 3AA2, after adsorption and co-adsorption the χ values decreased and increased. The adsorption of different NOM's on Ag (111) surface showed an increase in the values of χ as shown in Table 1.The higher the value of ω, the higher the electrophilic power of the investigated structure. Based on the above statement, from our calculated results we noticed that the electrophilicity index of Ag (111) surface was higher than that of adsorbates i.e. FA, AA1 and AA2, indicating a charge transfer from FA, AA1 and AA2 to Ag (111) surface.

To better elucidate the interaction between Ag (111) and NOM's it is worthwhile to study the electronic properties. For these purposes, analysis of total density of states (TDOS) is predominantly valuable. The TDOS of all NOM's on Ag (111) surface species in Figure 7 are drawn in the -30 to 4 eV ranges, in order to show the electronic structures near the Fermi level. TDOS of NOM's only and NOM with Ag (111) surface have also been studied and the data are shown in Figure 7 (a-d). Based on Figure 7 (a-d), upon interaction of Ag (111) surface with NOM's, no major changes in the energy states, the states kept the shape of Ag (111) surface which means there is not much done by the NOM's on Ag

(111) surface. Before adsorption in Figure S2 (Supporting document), it has been observed that the TDOS of isolated Ag (111) surface, FA, AA1 and AA2 have distinct peaks corresponding to separate energy levels. For the Ag (111) surface, the dominant peaks were observed at -6.8 eV, -5.2 eV, -4.1 eV and -2.8 eV which are all below Fermi level. For FA and AA1 the dominant peaks were observed at -7.1 eV, -5.2 eV, -2.8 eV and 0 eV which are all below Fermi level. In the case of AA2 the dominant peaks were observed at -7.2 eV, -5.0 eV and -2.1 eV which are all below Fermi level and 0.4, and 1.2 eV above Fermi level. After adsorption of FA, AA1, AA2 and a mixture of different NOM's on Ag (111) surface. Their TDOS demonstrates an alteration and the peaks move to the low energy level near the Fermi level even though the prominent peaks remain those of Ag (111) surface. After adsorption the dominant peaks were observed at -5.1 eV,-4.8 eV,-4.4 eV and 0 eV all below the Fermi level as shown in Figure 7. The small changes after adsorption in the TDOS of Ag (111) surface, FA, AA1 and AA2 show the interaction between the NOM's and Ag (111) surface. It can be concluded that the results of TDOS calculation show that after the interaction, the NOM's do not do much on the structure of silver, as confirmed by the results of after adsorption in Figure 7 (a-d). Results of TDOS in the gas phase are shown in supporting information Figure S3 (a-d) they are the same as the results of TDOS in water as a solvent.

In Figures 8-9 (a-i) PDOS plots for NOM's on Ag (111) surface calculated using DFT-D/GGA in water as a solvent, PDOS in gas phase are shown in Figures S4 and S5. PDOS in Figures 8-9 (a-i) show intense peaks below and one above Fermi level, prominent shoulder peaks corresponding to separate energy levels between -7.8 and -0.3 eV below the Fermi level and 0.3 eV above the Fermi level.

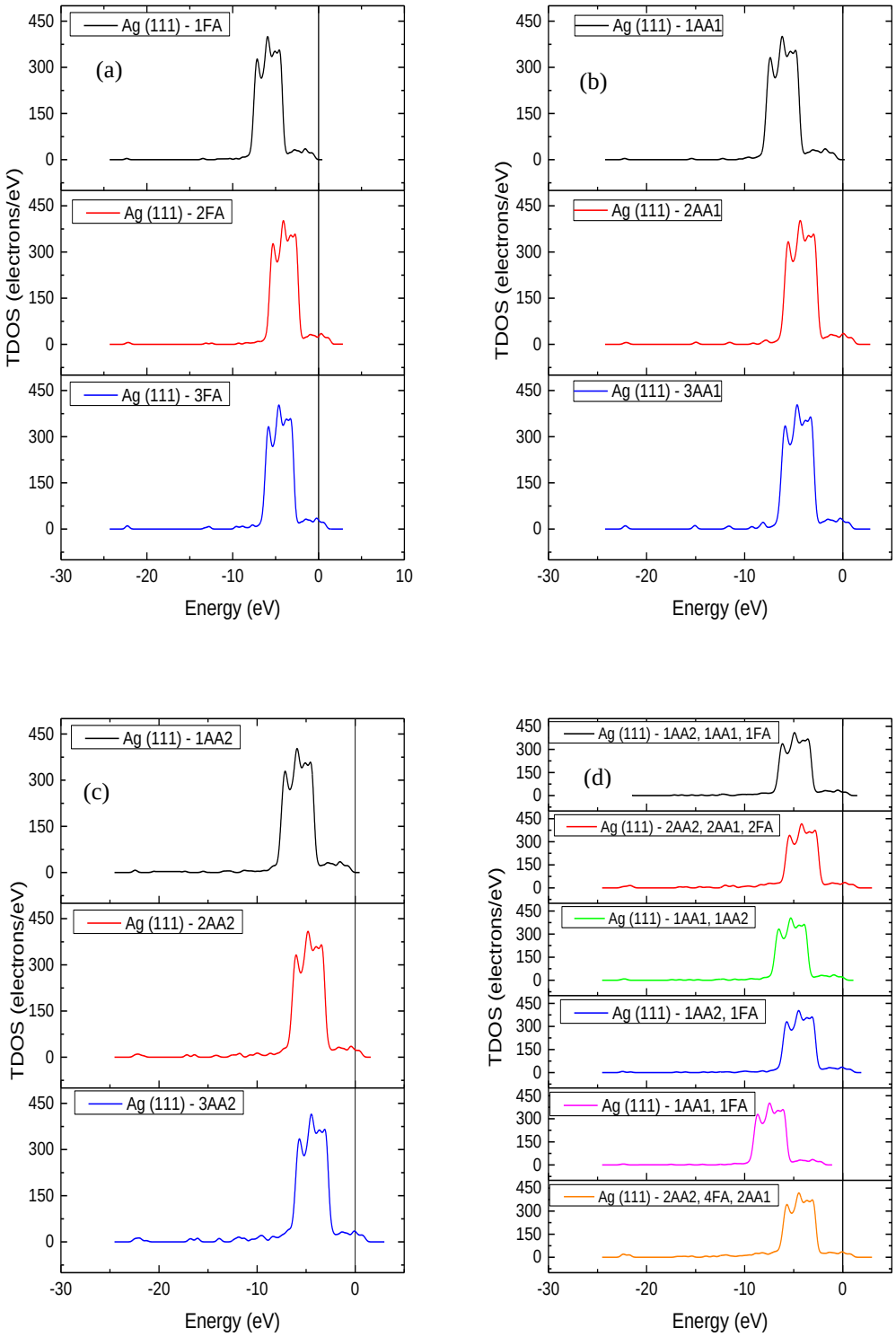

Figure 7: The total density of states (TDOS) in water as a solvent for (a) Ag (111)-1FA, Ag (111)-2FA and Ag (111)-3FA (b) Ag (111)-1AA1, Ag (111)-2AA1 and Ag (111)-3AA1 (c) Ag (111)- 1AA2, Ag (111)-2AA2 and Ag (111)-3AA2 and (d) Ag (111) surface with a mixture of NOM's. The Fermi level is indicated with a black vertical line.

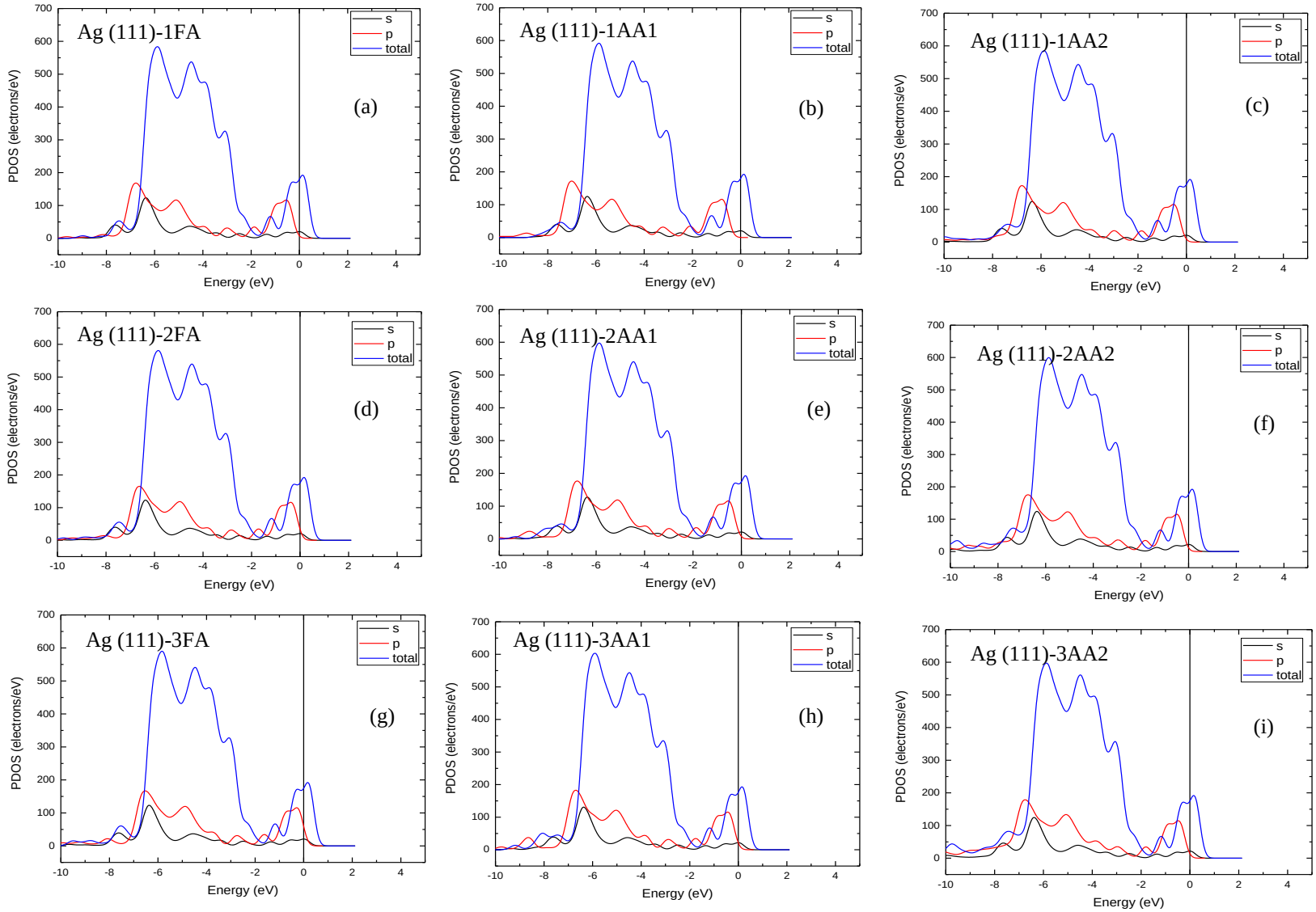

Figure 8: Projected density of states of NOM's on Ag (111) surface (a-f) in COSMO using DFT-D/GGA level of theory.

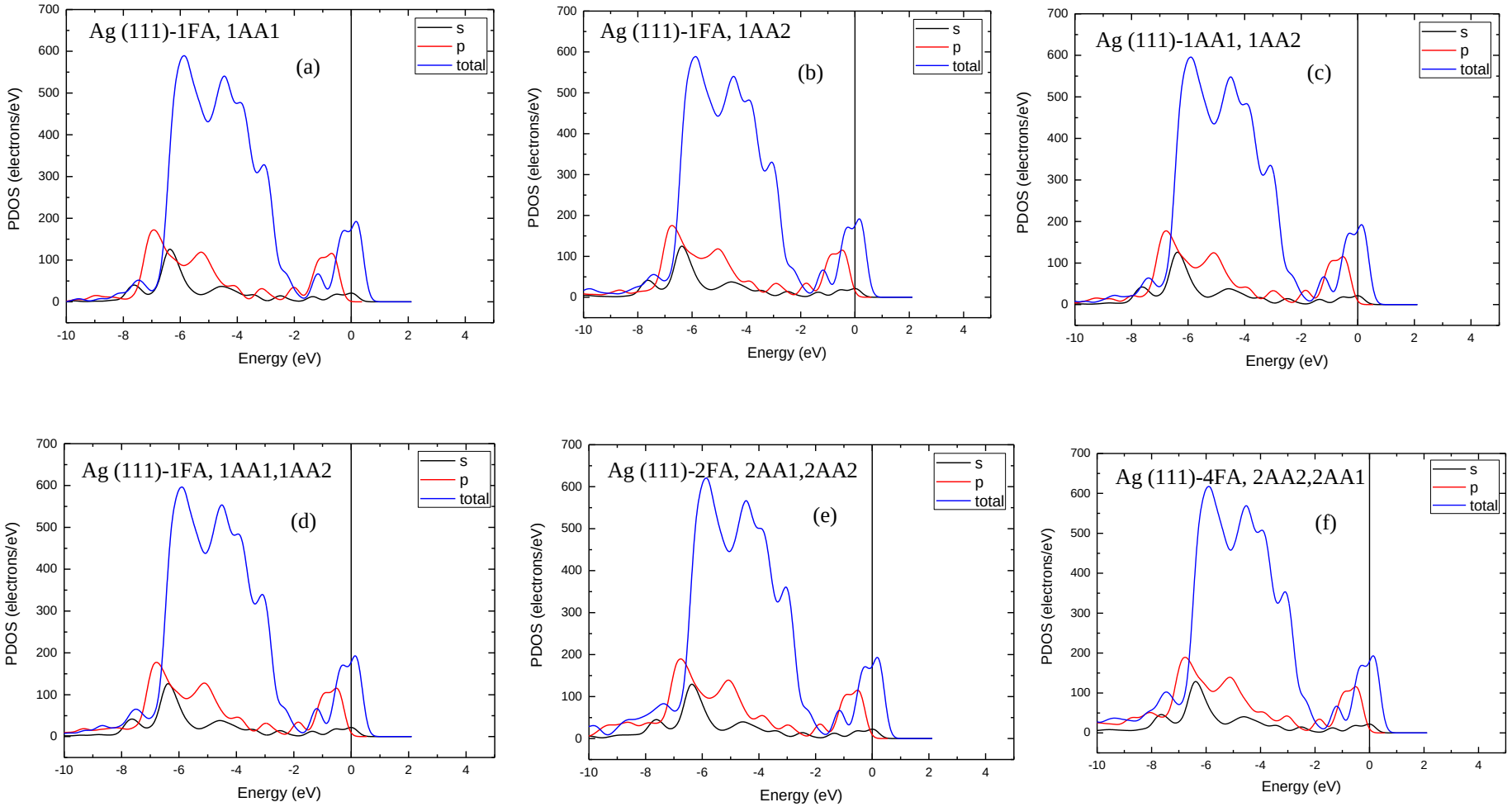

Figure 9: Projected density of states of NOM's on Ag (111) surface (a-f) in COSMO using DFT-D/GGA level of theory.

4. Conclusion

The main purpose of the work was to gain insight on the adsorption and co-adsorption of natural organic matter on Ag (111) surface. Thus the work aimed at answering the following questions: Can we adsorb more than one NOM on the Ag (111) surface? From this part of the work, it has been confirmed that well indeed, it is possible to co-adsorb a mixture of NOM's on Ag (111) surface. The adsorption and co-adsorption properties of one, more than one and a mixture of NOM's on Ag (111) surface using density functional theory dispersion-corrected (DFT-D) in the gas phase and water as a solvent have been investigated. The calculated adsorption energy results suggest that the interaction of 4FA, 2AA1 and 2AA2 molecules with Ag (111) surface is the strongest with most negative energy values (-6.54 and -3.84 eV) in both gas phase and COSMO. This reveals that it is the most stable system. The reason for the co-adsorption of 4FA, 2AA1 and 2AA2 molecules with Ag (111) surface to absorb more on Ag (111) surface can be attributed to the fact that when they are combined they have the highest molecular weight. In this section, the question of the competition between FA, AA1 and AA2 for the adsorption sites has been addressed; it is well known that different adsorbates with different properties will compete for the active sites when adsorbed on one Ag (111) surface. From the Table 3, it has been observed that from individual adsorption energies of FA, AA1 and AA2, the adsorbate with the highest adsorption energy will adsorb first on the Ag (111) surface. In our case AA2 from Table 3 has the highest adsorption energies compared to FA and AA1. It has been found that water as a solvent does not play a crucial role in enhancing the adsorption because the calculated adsorption energies in water as a solvent are not higher compared to adsorption energies in the gas phase. The global reactivity descriptors such as HOMO, LUMO, LUMO-HOMO, e.g. IP, EA, η and ω in the gas phase and water as a solvent were calculated. To better elucidate the adsorption characteristics of Ag (111) surface, total density of states (TDOS) analyses were performed, TDOS results showed little changes after the adsorption of low molecular weight NOM's on Ag (111) surface. The calculations have given a better understanding of the interaction of Ag (111) surface toward FA, AA1, and AA2 organics in the gas phase and in water as a solvent. In summary, the present work shows that it is possible to adsorb more than one NOM or a mixture of NOM's on one Ag (111) surface.

Acknowledgments

The authors acknowledge funding from the National Research Foundation (N.N.Nyangiwe), Council for Scientific and Industrial Research (N.N. Nyangiwe, C.N. Ouma). The computing and simulation resources from the Centre for High Performance Computing (CHPC), South Africa, are acknowledged.

References

[1] V. Stuttgen, H.E. Giffney, A. Anandan, A. Alabdali, C. Twarog, S.A. Belhout, M. O′ Loughlin, L. Podhorska, C. Delaney, N. Geoghegan, others, The UCD NanoSafety workshop (03/12/2018): Towards developing a consensus on safe handling of nanomaterials within the Irish university labs and beyond--A report, Nanotoxicology. 13 no 6 (2019) 717-732.

[2] K.-E. Kim, Y.S. Hwang, M.-H. Jang, J.H. Song, H.S. Kim, D.S. Lee, Development of a model (SWNano) to assess the fate and transport of TiO2 engineered nanoparticles in sewer networks, J. Hazard. Mater. 375 (2019) 290-296.

[3] D.T. Donia, M. Carbone, Fate of the nanoparticles in environmental cycles, Int. J. Environ. Sci. Technol. 16 (2019) 583–600.

[4] L. Wei, J. Lu, H. Xu, A. Patel, Z.-S. Chen, G. Chen, Silver nanoparticles: synthesis, properties, and therapeutic applications, Drug Discov. Today. 20 (2015) 595–601.

[5] C. Liu, W. Leng, P.J. Vikesland, Controlled evaluation of the impacts of surface coatings on silver nanoparticle dissolution rates, Environ. Sci. Technol. 52 (2018) 2726–2734.

[6] S. Yu, Y. Yin, J. Liu, Silver nanoparticles in the environment, Environ. Sci. Process. Impacts. 15 (2013) 78–92.

[7] M. Fazeli Sangani, G. Owens, A. Fotovat, Transport of engineered nanoparticles in soils and aquifers, Environ. Rev. 27 (2018) 43–70.

[8] J. Hedberg, E. Blomberg, I. Odnevall Wallinder, In the search for nano-specific effects of dissolution of metallic nanoparticles at freshwater-like conditions--a critical review, Environ. Sci. Technol. 53 no 8 (2019) 4030-4044.

[9] S.M. Louie, E.R. Spielman-Sun, M.J. Small, R.D. Tilton, G. V Lowry, Correlation of the physicochemical properties of natural organic matter samples from different sources to their effects on gold nanoparticle aggregation in monovalent electrolyte, Environ. Sci. Technol. 49 (2015) 2188–2198.

[10] B. Huang, Z.-B. Wei, L.-Y. Yang, K. Pan, A.-J. Miao, Combined Toxicity of Silver Nanoparticles with Hematite or Plastic Nanoparticles toward Two Freshwater Algae, Environ. Sci. Technol. 53 no 7 (2019) 3871-3879.

[11] C. Ma, X. Huangfu, Q. He, J. Ma, R. Huang, Deposition of engineered nanoparticles (ENPs) on surfaces in aquatic systems: a review of interaction forces, experimental approaches, and influencing factors, Environ. Sci. Pollut. Res. 25 (2018) 33056–33081.

[12] D. Arenas-Lago, F.A. Monikh, M.G. Vijver, W.J.G.M. Peijnenburg, Dissolution and aggregation kinetics of zero valent copper nanoparticles in (simulated) natural surface waters:Simultaneous effects of pH, NOM and ionic strength, Chemosphere. 226 (2019) 841–850.

[13] F. Zhang, Z. Wang, S. Wang, H. Fang, D. Wang, Aquatic behavior and toxicity of polystyrene nanoplastic particles with different functional groups: Complex roles of pH, dissolved organic carbon and divalent cations, Chemosphere. 228 (2019) 195–203.

[14] A.A. Keller, W. Vosti, H. Wang, A. Lazareva, Release of engineered nanomaterials from personal care products throughout their life cycle, J. Nanoparticle Res. 16 (2014) 2489.

[15] K.L. Garner, A.A. Keller, Emerging patterns for engineered nanomaterials in the environment: a review of fate and toxicity studies, J. Nanoparticle Res. 16 (2014) 2503.
[16] J.R. Lead, G.E. Batley, P.J.J. Alvarez, M.-N. Croteau, R.D. Handy, M.J. McLaughlin, J.D. Judy, K. Schirmer, Nanomaterials in the Environment: Behavior, Fate, Bioavailability, and Effects—An Updated Review, Environ. Toxicol. Chem. 37 no 8 (2018) 2029-2063.
[17] B. Wang, J. Nisar, R. Ahuja, Molecular simulation for gas adsorption at NiO (100) surface, ACS Appl. Mater. Interfaces. 4 (2012) 5691–5697.
[18] T.M. Benn, P. Westerhoff, Nanoparticle silver released into water from commercially available sock fabrics, Environ. Sci. Technol. 42 (2008) 4133–4139.
[19] M. Dickinson, T.B. Scott, The application of zero-valent iron nanoparticles for the remediation of a uranium-contaminated waste effluent, J. Hazard. Mater. 178 (2010) 171–179.
[20] S.J. Klaine, P.J.J. Alvarez, G.E. Batley, T.F. Fernandes, R.D. Handy, D.Y. Lyon, S. Mahendra, M.J. McLaughlin,J.R Lead, Nanomaterials in the environment: Behavior, fate, bioavailability, and effects, Environ. Toxicol. Chem. 27 no 9 (2008) 1825-1851.

[21] M.C. Surette, J.A. Nason, Nanoparticle aggregation in a freshwater river: the role of engineered surface coatings, Environ. Sci. Nano. 6 no 2 (2019) 540-553.

[22] O.Francioso, E.Lopez-Tobar, A.Torreggiani, M. Iriarte, S. Sanchez-Cortes, Stimulated Adsorption of Humic Acids on Capped Plasmonic Ag Nanoparticles Investigated by Surface-Enhanced Optical Techniques, Langmuir. 35 no 13 (2019) 4518-4526.

[23] D.P. Stankus, S.E. Lohse, J.E. Hutchison, J.A. Nason, Interactions between natural organic matter and gold nanoparticles stabilized with different organic capping agents, Environ. Sci. Technol. 45 (2010) 3238–3244.
[24] Z. Ban, Q. Zhou, A. Sun, L. Mu, X. Hu, Screening Priority Factors Determining and Predicting the Reproductive Toxicity of Various Nanoparticles, Environ. Sci. Technol. 52 (2018) 9666–9676.
[25] N.N. Nyangiwe, C.N. Ouma, N. Musee, Study on the interactions of Ag nanoparticles with low molecular weight organic matter using first principles calculations, Mater. Chem. Phys. 200 (2017) 270-279.
[26] N.N. Nyangiwe, C.N.M. Ouma, Modelling the adsorption of natural organic matter on Ag (111) surface: Insights from dispersion corrected density functional theory calculations, J. Mol. Graph. Model. 92 (2019) 313-319.
[27] B. Delley, Hardness conserving semilocal pseudopotentials, Phys. Rev. B. 66 (2002) 155125.
[28] J.P. Perdew, K. Burke, M. Ernzerhof, Generalized gradient approximation made simple, Phys. Rev. Lett. 77 (1996) 3865.

[29] A. Klamt, Conductor-like screening model for real solvents: a new approach to the quantitative calculation of solvation phenomena, J. Phys. Chem. 99 (1995) 2224–2235.

[30] M. Anafcheh, R. Ghafouri, Silicon doping of defect sites in Stone--Wales defective carbon nanotubes: A density functional theory study, Superlattices Microstruct. 60 (2013) 1–9.

[31] B. Wiley, Y. Sun, B. Mayers, Y. Xia, Shape-controlled synthesis of metal nanostructures: the case of silver, Chem. Eur. J. 11 (2005) 454–463.

[32] S. Pal, Y.K. Tak, J.M. Song, Does the antibacterial activity of silver nanoparticles depend on the shape of the nanoparticle? A study of the gram-negative bacterium Escherichia coli, Appl. Environ. Microbiol. 73 (2007) 1712–1720.

[33] J.R. Morones, J.L. Elechiguerra, A. Camacho, K. Holt, J.B. Kouri, J.T. Ram\'\irez, M.J. Yacaman, The bactericidal effect of silver nanoparticles, Nanotechnology. 16 (2005) 2346.

[34] N.I.B. Hartmann, L.M. Skjolding, S.F. Hansen, A. Baun, J. Kjølholt, F. Gottschalk, Environmental fate and behaviour of nanomaterials: New knowledge on important transfomation processes. Copenhagen K: Danish Environmental Protection Agency, (2014). 115 p. (Environmental Project; No. 1594).

[35] V. Timón, M.L. Senent, M. Hochlaf, Structural single and multiple molecular adsorption of CO2 and H2O in zeolitic imidazolate framework (ZIF) crystals, Microporous Mesoporous Mater. 218 (2015) 33–41.

[36] A. Nalaparaju, X.S. Zhao, J.W. Jiang, Molecular understanding for the adsorption of water and alcohols in hydrophilic and hydrophobic zeolitic metal- organic frameworks, J. Phys. Chem. C.114 (2010) 11542–11550.

[37] V.S. Sastri, J.R. Perumareddi, Molecular orbital theoretical studies of some organic corrosion inhibitors, Corrosion. 53 (1997) 617–622.

[38] A.S. Rad, Al-doped graphene as a new nanostructure adsorbent for some halomethane compounds: DFT calculations, Surf. Sci. 645 (2016) 6–12.

[39] A.S. Rad, E. Abedini, Chemisorption of NO on Pt-decorated graphene as modified nanostructure media: a first principles study, Appl. Surf. Sci. 360 (2016) 1041–1046.